## **Use of Artificial Neural Networks to Estimate Installation Damage of Nonwoven Geotextiles**

Ehsan Amjadi Sardehaei<sup>\*1</sup>, Gholamhosein Tavakoli Mehrjardi<sup>1</sup>

1. Department of Civil Engineering, Faculty of

Engineering, Kharazmi University, Tehran, Iran.

Received: 3 April 2017 Revised: 17 Oct 2017

### **Abstract**

This paper presents a feed-forward back-propagation neural network model to predict the retained tensile strength and design chart to estimate the strength reduction factors of nonwoven geotextiles due to the installation process. A database of 34 full-scale field tests was utilized to train, validate and test the developed neural network and regression model. The results show that the predicted retained tensile strength using the trained neural network is in good agreement with the results of the test. The predictions obtained from the neural network are much better than the regression model as the maximum percentage of error for training data is less than 0.87% and 18.92%, for neural network and regression model, respectively. Based on the developed neural network, a design chart has been established. As a whole, installation damage reduction factors of the geotextile increases in the aftermath of the compaction process under lower as-received grab tensile strength, higher imposed stress over the geotextiles, larger particle size of the backfill, higher relative density of the backfill and weaker subgrades.

**Keywords:** Artificial neural networks (ANNs), Regression model; Nonwoven geotextiles, Retained tensile strength, strength reduction factor.

<sup>\*</sup>Corresponding author Amjadi.Ehsan@yahoo.com

# [ DOR: 20.1001.1.22286837.1398.13.5.3.2

### Introduction

Geotextiles are one of the main groups of geosynthetics that have been extensively applied in soil reinforcement of geotechnical projects such as embankments over soft subgrades, road construction, slopes, retaining walls and buried pipelines [1-4].

The primary reduction factor applied to the tensile strength of the geotextiles is due to installation damage. The stresses applied to the subgrade and the geotextile during construction may be much greater than those applied in service. Therefore, the selection of the geotextile in roadway applications is usually governed by the anticipated construction stress. In other words, the geotextile must survive the construction operations if it is to perform its intended function [5].

In visual inspection, two methods including the scanning electron microscopy (SEM) and naked eye inspection are applicable. Different modes of installation outcomes such as cutting, fraying, very fine-grained particles sediment in texture, fiber separation, holes and squeeze of geotextiles by larger soil particles are investigated. The results of some previous studies, observed by the visual inspection, are summarized in Table 1 [6-10].

Recently, there has been a great resurgence of research in neural network classifiers. ANNs are defined as computing systems made up of many simple, highly interconnected processing elements called neurons. The networks are represented by connective weights between the neurons. The process of determining these weights is called training or learning and depends on the presentation of as many reliable training patterns as possible. ANNs are capable to perform an amount of generalization from the data entries on which they are trained [11].

Table 1. Result summary of researchers in visual inspection by using the SEM and naked eyes methods

Inspection type	Researcher	Results			
	Greenwood and Brady (1992)	Generally involves cutting, fraying (decay) and erosion			
	Pinho-Lopes and Lopes (2013)	Generally involves cutting and puncture have been observed.			
SEM	Rosete et al. (2013)	Fine-grained particles sediment in texture of geotextile.  The impact of larger load is more understandable.			
	Carlos et al. (2015)	Finer soils (silty sand and sandy silt) created less visible changes (without fiber separation, cutting and erosion).  Granular soils (sand and gravel) exerted fiber			
		erosion  Generally involves cutting and puncture have been observed.  Fine-grained particles sediment in texture of geotextile.  The impact of larger load is more understandable.  Finer soils (silty sand and sandy silt) created less visible changes (without fiber separation, cutting			
Naked eyes	Watn et al. (1998)	Using the lighter compactor ended in a significant			

The current paper by using the experimental data investigates the feasibility of using ANNs to evaluate the retained tensile strength of nonwoven geotextiles due to the installation process. Then, comparisons between predicted results of the trained neural network, regression model and those obtained from experimental data are presented. Finally, to estimate installation damage reduction factor of nonwoven geotextiles, a design chart is established based on the developed neural network.

### **Description of experimental model**

A series of full-scale field tests were carried out to investigate installation damage of nonwoven geotextiles in unpaved roads. The studied parameters consisted of backfill median grain size ( $D_{50} = 3$ , 6, 12 and 16 mm), two types of subgrade namely "fine-grained subgrade, FS" and "coarse-grained subgrade, CS", three types of needle-punched nonwoven geotextiles (representatives of Classes 1, 2 and 3 by following AASHTO M 288-08 [12]), two different relative densities ( $D_r$ =70%= $C_1$  (median dense) and 90%= $C_2$  (very dense). The technical properties of backfill and subgrade materials and also the utilized geotextiles are tabulated in Tables 2 and 3, respectively [13-16].

Table 2. Physical properties of backfill and subgrade materials

	Backfill materials				Subgrade	
Description	Cond	Gravel	Gravel	Carrel	CS	FS
Description	Sand	6 mm		Gravel 16 mm	0-2	0-25
	3 mm		12 mm		mm	mm
Coefficient of uniformity, Cu	2.125	2.14	1.33	1.27	10.95	7.16
Coefficient of curvature, Cc	1.19	1.08	0.95	0.96	2.86	1.55
Median grain size, D <sub>50</sub> (mm)	3.1	5.9	12.5	16.5	3.65	1.00
Specific gravity, Gs	2.419	2.494	2.546	2.604		
CBR soaked (%)					49	27
Moisture content (%)	Dry	Dry	Dry	Dry	5	5
Classification (USCS)	SP	GP	GP	GP	SW	SW

Table 3. Engineering properties of the geotextiles used

Description	Test methods	$GT_3$	$GT_2$	$GT_1$
Mass per unit area (g/m²)	ASTM D 5261-10	292	319	508
Grab tensile strength (N)	ASTM D 4632-15a	650	800	1350
Grab elongation (%)	ASTM D 4632-15a	> 50	> 50	> 50
Trapezoidal tear strength (N)	ASTM D 4533-15	310	385	600
CBR puncture (N)	ASTM D 6241-14	900	1500	2500
Class (AASHTO M 288-08)		3	2	1

To simulate the installation process of geotextiles in unpaved roads, the geotextiles were installed over the constructed subgrades and buried beneath the backfill materials with desired relative density. To compact the backfill, a walk-behind tandem vibratory roller was used statically. At the end of the compaction process, the backfill was removed carefully to ensure that the geotextiles could be exhumed without any additional damage. Figure 1 shows the schematic representation of the test setup.

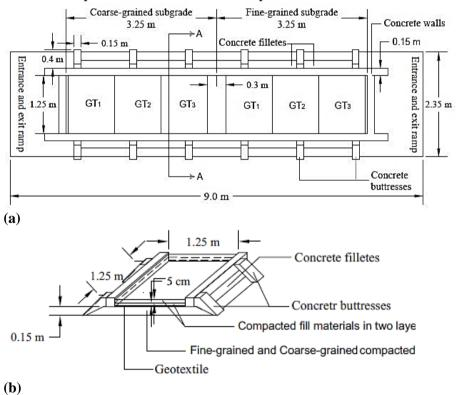


Figure 1. Schematic representation of the test setup (a) plan (b) section A-A [17], [27]

# [ Downloaded from jeg.khu.ac.ir on 2024-04-30

# Results and discussions on artificial neural networks Inputs and outputs of the network

In the design of ANNs structure for predicting the retained tensile strength of nonwoven geotextiles due to installation process, the input layers consists of as-received geotextile grab tensile strength  $(T_0)$ , imposed stress over the geotextiles during installation  $(\sigma)$ , median grain size of backfill materials  $(D_{50})$ , subgrade's CBR and relative density of backfills  $(D_r)$ . The output layer consists of the retained tensile strength of geotextiles. The range of input parameters of the data used to train the ANNs is given in Table 4.

Table 4. Range of input parameters of the experimental data used to train the ANNs

input parameters	Range of parameter
as-received geotextile tensile strength (kN)	0-1.35
imposed stress over the geotextiles (kPa)	68-70
median grain size of the backfill (m)	0.003-0.016
Subgrade's CBR (%)	27-49
relative density of backfills (%)	70-90

### Transfer function and scaling of the training data

For better network performance, the input and output data pairs were subjected to the scaling process before being used in the network operation. This is because the compiled raw training data for different parameters can vary significantly in their actual values. When such non-scaled data are directly used in the training procedure, the network could exhibit ill-conditioning.

Also, the selection of transfer functions plays an important role in

ANNs problems. Among the several different types of transfer functions, the tan-sigmoid and pure-linear transfer functions were used in this study. The output of the network (retained tensile strength of geotextiles) is subjected to an inverse scaling to return the actual quantities of the output parameters. Also, the neural network available in MATLAB version 8.5.0 [18] was utilized to construct the proposed neural networks. A package of neural network has been used to model the problem using backpropagation neural networks [19].

### **Training of ANNs**

The training of the neural network is carried out using the training dataset. Testing and monitoring of the developed neural network during the training stage is performed by computing the mean squared error (MSE) overall training, validation and testing datasets. After each of the training iteration, the obtained weights are used to predict the corresponding retained tensile strength to the input parameters of the training, validation and testing datasets. The mean squared error was calculated for each pattern as the difference between the retained tensile strength obtained from the trained neural network and the corresponding experimental retained tensile strength. For neural networks, several architectures of ANN models were examined by varying the number of hidden layers, the number of neurons in each hidden layer and the training function parameters. The best neural network was identified after several trials to have

four layers. These are included with an input layer of five neurons  $(T_0, \sigma, D_{50}, CBR)$  and,  $D_r$ , an output layer of one neuron retained tensile strength and also two hidden layers. It is noted that the number of neurons in each hidden layer is trained once the error of the network reaches a minimum value. Thus, investigations confirmed that the optimum number of neurons in first and second hidden layers was 10 neurons for predicting of retained tensile strength. The ANNs structure used for training of retained tensile strength is shown in Figure 2. It should be noted that two datasets are generated: one was used as a training dataset which used to train and another was used as a test dataset to evaluate the performance of a model on data not considered during the training stage. Hence, 34 experimental data were available which among them 24 data are allocated (randomly chosen) for training and 10 data are used for testing and validating the network during the training.

### **Evaluation of the training stage**

To show the advantage of ANNs as the new technology compared to the mathematical model, the regression analysis was carried out to fit the training dataset. Equations (1) and (2) illustrate dimensional and non-dimensional relationships to interpolate and extrapolate the effective parameters and retained tensile strength of the geotextiles  $(T_{ID})$ . According to Equation (1), the major physical parameters influencing the retained tensile strength  $(T_{ID})$  can be summarized in

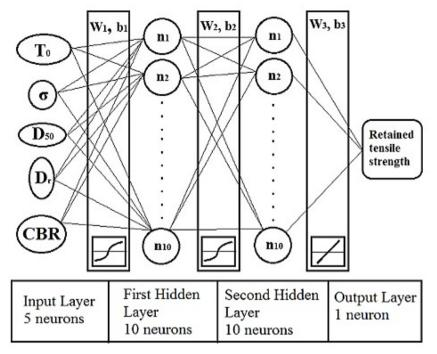


Figure 2. Schematic of ANNs structure for training of retained tensile strength

as-received geotextile tensile strength  $(T_0)$  in Newton, transferred stress over the geotextiles level during installation  $(\sigma)$  in Pascal, median grain size of backfill materials  $(D_{50})$  in meter, relative density of backfills  $(D_r)$  in term of percentage and subgrade CBR in term of percentage. Equation (1) comprises 5 parameters which two of them have fundamental dimensions (i.e. length and force). Therefore, Equation (1) can be reduced to 3 independent parameters and substituted with Equation (2).

$$T_{ID} = f(T_0, \sigma, D_{50}, D_r, CBR)$$
 (1)

$$\frac{T_{ID}}{T_0} = f(\frac{T_0}{\sigma D_{50}^2}, D_r, CBR)$$
 (2)

To determine the best-fitted equation, great numbers of linear and non-linear regression models were examined to select the best subset of predictors. Among all possibilities, natural-logarithm function (Eq. 3) was selected to estimate retained tensile strength, resulting in the maximum value of the coefficient of determination; R<sup>2</sup> and minimum value of mean squared error.

$$T_{ID} = [0 \cdot 875 + 0 \cdot 019 \ln \left(\frac{T_0}{\sigma D_{50}^2}\right) - 0 \cdot 029 \ln(D_r) + 0 \cdot 018 \ln(CBR)] \times T_0$$
 (3)

Figure 3 comprises the obtained retained tensile strength from experimental data and those obtained from the trained neural network and regression model. It is shown that there is no serious out-layer point around the 0% error line for ANNs compared to the regression results for retained tensile strength. Table 5 gives statistical parameters to evaluate the performance of the trained ANNs and regression method for retained tensile strength. The absolute average percentage of error (e<sub>ave</sub>) in the estimation of retained tensile strength was 0.12% with the trained ANN and 4.99% with the regression method, whereas the maximum percentage of error (e<sub>max</sub>) using the trained ANN and the regression method were 0.87% and 18.92%, respectively. The value of R<sup>2</sup> for the ANN is greater than that of obtained from the regression method for retained tensile strength as indicated in Table 5. For example, the obtained values of R<sup>2</sup> indicate that the model as fitted explains 99.99% and 97.61% of the

variability in retained tensile strength for the ANN and regression method, respectively. Also, the value of MSE for the ANN is less than the regression method. Besides, these statistical parameters show that the predictions obtained from both the trained ANN and regression method are good agreement with experimental results, but trained ANN are better than those obtained from the regression method.

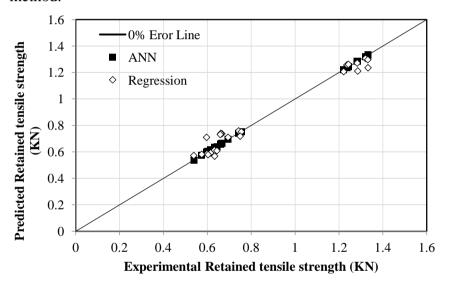


Figure 3. Comparison of trial ANNs and Regression predicted values with experimental results

Table 5. Statistical parameters for measuring the performance of the trained ANNs and regression model

Parameter		Method	e <sub>ave</sub>	e <sub>max</sub>	$\mathbb{R}^2$	MSE
Retained	tensile	ANNs	0.12	0.87	0.9999	0.00000255
strength		Regression	4.99	18.92	0.9761	0.002358

 $e_{ave}$ , the absolute average percentage of error in the predicted values;  $e_{max}$ , the maximum percentage of error in the predicted values;  $\mathbf{R}^2$ , the coefficient of determination; MSE, the mean squared of error.

### Verification of the trained model

For verification of the proposed model, the model has been evaluated with 10 additional experimental data that were not used in training the model. Table 6 demonstrates statistical parameters to investigate performance of the trained ANNs and regression method for retained tensile strength. The values of statistical parameters (e<sub>ave</sub>, e<sub>max</sub>, R<sup>2</sup>, MSE) calculated for the ANN and the regression model are close to each other, as indicated in Table 6. By comparison of the estimated statistical parameters for the ANN and regression models for all data used in training and test stages, it can be concluded that the predicted value of retained tensile strength using the trained ANN and the regression method are good agreement with experimental results. Furthermore, it is well understood that the ANN predictions were closer to the experimental results than those for the regression model.

Table 6. Statistical parameters for measuring the performance of the ANNs and regression model for data not used in training stage

Parameter	Method	e <sub>ave</sub>	e <sub>max</sub>	$\mathbb{R}^2$	MSE
Retained tensile	ANNs	3.86	7.3	0.98	0.00119
strength	Regression	2.07	5.93	0.99	0.00095

 $e_{ave}$ , the absolute average percentage of error in the predicted values;  $e_{max}$ , the maximum percentage of error in the predicted values;  $R^2$ , the coefficient of determination; MSE, the mean squared of error.

### Limitation and applicability of the proposed model

ANNs offer a fundamentally different approach to modeling different engineering problems. But, for predicting the model, the conditions and limitations of each problem should be considered. To clarify the proposed ANNs, some points are necessary to discuss as follows:

The ANN model trained by experimental data is established for only one type of roller (as compacting machinery), one type of geotextile from a manufacturing process point of view (needlepunched nonwoven) and similar backfill thickness. Hence, it should be noted that the effect of some other parameters, which have not been investigated, should be considered. Thus, the proposed neural network can be applied by considering the above limitations.

The ANNs database is dynamic; therefore, the network will be able to access a richer training set as the experimental or fieldwork continues. More complex path experimental or field tests on various conditions such as different rollers, various types of geotextile and backfill thickness to expand the capabilities of neural a network model can be very useful.

The results indicate that there is a good agreement between predicted and experimental results in the above range of input variable parameters. But it is important to note that complete agreement between the experimental trends and those inferred from the model should not be expected. This refers to the uncertainty and inaccuracy of the experimental data.

It can be expected that, with an increase in the size and diversity of the database for the training of the ANNs, it would be possible to obtain more robust models for the prediction of retained tensile strength, studying the effects of input variable parameters in a wider variation range.

### Design chart results and discussion

Based on the developed neural network, the values of  $T_{ID}$  were obtained and then, by dividing them to the corresponding  $T_0$ , the values of installation damage reduction factor of geotextiles (RF<sub>ID</sub>) were determined. Thus, a design chart has been produced and shown in Figure 4, to estimate installation damage reduction factor of geotextiles (RF<sub>ID</sub>) respect to the variation of the studied parameters. Also, it should be noted that in ratio of  $\sigma$  (D<sub>50</sub> D<sub>r</sub>)<sup>2</sup> / T<sub>0</sub>,  $\sigma$  is transferred stress at the level of geotextile in (Pa or kPa); D<sub>50</sub> is medium grain size of the backfill in (m); D<sub>r</sub> is relative density of the backfill in percent and T<sub>0</sub> is as-received grab tensile strength of geotextiles in (N or kN).

Accordingly, reduction factors due to the installation of geotextiles in the backfill were obtained 1~1.42. This range of values is in the line with that stated in FHWA-NHI-10-024 [20], suggesting RD<sub>ID</sub>=1.1~1.4 for nonwoven geotextiles in backfill with maximum grain size 20 mm. As can be seen, the transferred stress at the level of geotextile can be the resultant of the backfill's weight and stress propagated by the compactor energy, having a direct role in

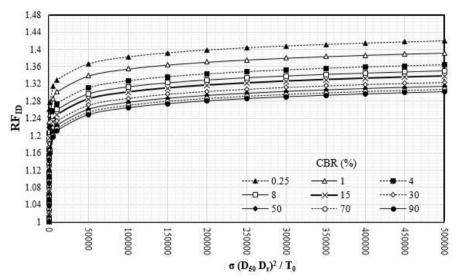


Figure 4. Design chart for tensile strength reduction factor due to installation damage

installation damage. Consequently, it is suggested that in constructions, lighter compactors and a thicker cover of the backfill materials over the geotextile should be utilized, as much as possible [6, 7, 10, 21, 22, 23, 24]. Also, increasing the relative density of backfill materials increased the installation damage reduction factor and it can be concluded that the variations of installation damage reduction factors of geotextiles due to transferred stress and relative density are the same order. Increasing the soil particle size intensifies the installation damage of the geotextiles. Increasing the grain size could increase the chance of stone-stone interactions, tending to transfer more stress onto the geotextiles. Expectedly, geotextile class 1 due to its greater thickness, gained less impact from the installation

process. Therefore, using high-survivability geotextiles (i.e. class 1 per AASHTO M288-08 [12]) in backfills containing large particle size is highly recommended. In this regard, FHWA-NHI-10-024 [20] focused on the grain size of backfill and geotextile's type to suggest reduction factor due to installation damage. Furthermore, the results confirm the continues degradation of geotextiles in the aftermath of being in the neighborhood of weaker subgrades. Weak subgrade directly affects the amount of extension in the geotextile layer under imposed stress. It means that reduction in CBR of the subgrade ended in the occurrence of more settlements beneath the geotextile, exerting more tension through its plane and thereby causing severe damage. FHWA HI-95-038 [5] recommends that higher survivability geotextiles should be used when the subgrade has low shear strength.

### **Summary and conclusion**

The selection of the geotextile in roadway applications is usually governed by the anticipated construction stress. Since the tensile strength of reinforcements is a key parameter in the performance of reinforced soil [25-27], therefore, the estimation of the reduction factor of tensile strength due to installation damage is essential. The current paper, by using the experimental data, investigates the feasibility of using ANNs to evaluate the retained tensile strength of nonwoven geotextiles due to the installation process. The results of the study, as applied to the geotextile

installations, can be summarized as follows:

The comparisons of the statistical parameters of the ANN and regression for all data used in training and test stages imply that the predicted value of retained tensile strength using the trained ANN is more adjustable than the regression model.

The strength reduction factor is increased owing to higher backfill compaction. This confirms the continued weakness of geotextiles in the aftermath of transferred stress intensification.

Increasing the soil particle size intensifies the installation damage of the geotextiles. Increasing the grain size could increase the chance of stone-stone interactions, tending to transfer more stress onto the geotextiles.

Using geotextiles with higher as-received grab tensile strength (increasing the geotextiles Class from 3 to 1) results in a decrease of installation damage.

The installation damage of geotextiles is more pronounced as the subgrades' CBR increases, probably due to its direct effect on the amount of extension in the geotextile layer under imposed stress.

	Nomenclature
$C_{u}$	Coefficient of uniformity
$C_c$	Coefficient of curvature
D <sub>50</sub> (mm)	Median grain size
$G_{s}$	Specific gravity of soil
CS	Coarse-grained subgrade

FS	Fine-grained subgrade
$T_0$	As-received Grab tensile strength of the geotextiles
σ	Transferred stress at the level of geotextile
$D_{r}$	Backfill's relative density
CBR	Subgrade' CBR
$RF_{ID}$	Installation damage reduction factor of geotextile
$T_{\mathrm{ID}}$	Retained Grab tensile strength of the geotextiles
$T_0 / (\sigma D_{50}^2)$	Dimensionless parameter

### **List of Tables:**

Table 1	Result summary of researchers in visual inspection by using the SEM and naked eyes methods				
Table 2	Physical properties of backfill materials and subgrades				
Table 3	Engineering properties of the geotextiles used				
Table 4	le 4 Range of input parameters of the experimental data used to train the ANNs				
Table 5	Statistical parameters for measuring the performance of the trained ANNs and regression model				
Table 6	Statistical parameters for measuring the performance of the ANNs and regression model for data not used in training stage				

### **List of Figures:**

Figure 1	1 Schematic representation of the test setup (a) plan (b) section A-A		
Figure 2	Schematic of ANNs structure for training of retained tensile strength		
Figure 3	Comparison of trial ANNs and Regression predicted values with experimen		
	results		
Figure 4	Design chart for tensile strength reduction factor due to installation damage		

### References

- Wang L., Zhang G., Zhang J. M., "Centrifuge model tests of geotextilereinforced soil embankments during an earthquake", Geotextiles and Geomembranes, Vol. 29 (2011) 222-232.
- Tavakoli Mehrjardi Gh., Moghaddas Tafreshi S. N., Dawson A. R., "Pipe response in a geocell reinforced trench and compaction considerations", Geosynthetics International, Vol. 20 (2013) 105-118.

[ DOR: 20.1001.1.22286837.1398.13.5.3.2 ]

- Portelinha, F. H. M., Zorenberg J. G., Pimental V., "Field performance of retaining walls reinforced with woven and nonwoven geotextiles", Geosynthetics International, Vol. 21 (2014) 270-284.
- Hosseinpou I., Almeida M. S. S., Riccio M., "Full-scale load test and finite-element analysis of soft ground improved by geotextile-encased granular columns". Geosynthetics International, Vol. 22 (2015) 428-438.
- Federal Highway Administration, "Geosynthetic design and construction guidelines", FHWA-HI-95-038 (1998), Washington, USA.
- Greenwood J. H., Brady K. C., "Geotextiles in aggressive soils".
   Construction and Building Materials, Vol. 6 (1992) 15-18.
- Pinho-Lopes M., Lopes M. L., "Tensile properties of geosynthetics after installation damage", Environmental Geotechnics, Vol. 1 (2013) 161-178.
- Rosete A., Lopes P. M., Pinho-Lopes M., Lopes M. L., "Tensile and hydraulic properties of geosynthetics after mechanical damage and abration laboratory tests", Geosynthetics International, Vol. 20 (2013) 358-374.
- Carlos D. M., Pinho-Lopes M., Carneiro J. R., Lopes M. L., "Effect of soil grain size distribution on the mechanical damage of nonwoven geotextiles under repeated loading", International Journal of Geosynthetics and Ground Engineering, (2015) 1-9.
- Watn A., Eiksund G., Knutson A., "Deformation and damage of nonwoven geotextiles in road construction", Sixth International Conference on Geosynthetics, (1998) 933-938.
- 11. Moghaddas Tafreshi S. N., Tavakoli Mehrjardi Gh., "The use of neural

- network to predict the behavior of small plastic pipes embedded in reinforced sand and surface settlement under repeated load", Engineering Applications of Artificial Intelligence, Vol. 21 (2008) 883-894.
- 12. American Association of State Highway and Transportation Officials (AASHTO) "Standard Specification for Geotextile Specification for Highway Applications", AASHTO M288-08 (2008), Virginia, USA.
- 13. American Society for Testing and Materials (ASTM) "Standard Test Method for Measuring Mass per Unit Area of Geotextiles", ASTM D 5261-10 (2010), West Conshohocken, PA, USA.
- 14. American Society for Testing and Materials (ASTM) "Standard Test Method for Grab Breaking Load and Elongation of Geotextiles", ASTM D 4632-15 (2015), West Conshohocken, PA, USA.
- 15. American Society for Testing and Materials (ASTM) "Standard Test Method for Trapezoidal Tearing strength of Geotextiles", ASTM D 4533-15 (2015), West Conshohocken, PA, USA.
- 16. American Society for Testing and Materials (ASTM) "Standard Test Method for Static Puncture Strength of Geotextiles and Geotextile-Related Products Using a 50-mm Probe", ASTM D 6241-14 (2014), West Conshohocken, PA, USA.
- 17. Tavakoli Mehrjardi Gh., Amjadi Sardehaei E., "Design graphs to estimate reduction factor of nonwoven geotextiles due to installation process", European Journal of Environmental and Civil Engineering, Vol. 22 (2017) 1-14.
- 18. MathWorks Inc., "MATLAB the Language of Technical Computing", Version 8, (2015) Natick, MA, USA.

[ DOR: 20.1001.1.22286837.1398.13.5.3.2

- 19. Hagan M. T., Dermuth H. B., Beale M., "Neural Network Design". PWS Publishing Co (1995), Boston, MA, USA.
- Berg R. R., Christopher B. R., Samtani N. C., "Design of mechanically stabilized earth walls and reinforced soil slopes Vol. (1)", FHWA NHI-10-024 (2009), Federal Highway Administration, Washington, USA.
- 21. Watts G. R. A., Brady K. C., "Geosynthetics-installation damage and the measurement of tensile strength", Fifth International Conference on Geotextiles, Geomembranes and Related Products, Singapore, (1994) 1159-1164.
- 22. Elvidge C. B., Raymond G. P., "Laboratory survivability of nonwoven geotextiles on open-graded crushed aggregate", Geosynthetics International, Vol. 6 (1999) 93-117.
- 23. Hufenus R., Rüegger R., Flum D., Sterba I.J., "Strength reduction factors due to installation damage of reinforcing geosynthetics". Geotextiles and Geomembranes, Vol. 23 (2005) 401-424.
- 24. Koerner G. R., Koerner R. M., "The installation survivability of geotextiles and geogrids", Fourth International Conference on Geotextiles, Geomembranes and Related Products, Den Haag, (1990) 597-602.
- 25. Tavakoli Mehrjardi Gh., Moghaddas Tafreshi S. N., Dawson A. R., "Combined use of geocell reinforcement and rubber-soil mixtures to improve performance of buried pipes", Journal of Geotextiles and Geomembranes, Vol 34(4) (2012) 116-130.
- 26. Tavakoli Mehrjardi Gh., Ghanbari A., Mehdizadeh H., "Experimental study on the behaviour of geogrid-reinforced slopes with respect to

- aggregate size", Geotextiles and Geomembranes, Vol. 44 (2016) 862-871.
- 27. Amjadi Sardehaei E., Tavakoli Mehrjardi Gh., Dawson A., "Full-scale investigations into installation damage of nonwoven geotextiles", Geomechanics and Engineering, An international journal, Vol. 17 (2019) 81-95.
- 28. Tavakoli Mehrjardi Gh., Khazaei M., "Scale Effect on the Behavior of Geogrid-Reinforced Soil under Repeated Loads", Geotextiles and Geomembranes, Vol. 45(6) (2017) 603-615.